Battery internal resistance estimation using a battery balancing system based on switched capacitors

Cristina González Moral
Electrotécnica Industrial y Naval, S.L. (ELINSA)
La Coruña, Spain
cgonzalez@elinsa.org

Diego Fernández Laborda
University of Oviedo
Gijón, Spain
dflaborda@uniovi.es

Lidia Sánchez Alonso
University of Oviedo
Gijón, Spain
uo250173@uniovi.es

Juan Manuel Guerrero
University of Oviedo
Gijón, Spain
guerrero@uniovi.es

Daniel Fernández
University of Oviedo
Gijón, Spain
fernandezalodaniel@uniovi.es

Carlos Rivas
Electrotécnica Industrial y Naval, S.L. (ELINSA)
La Coruña, Spain
crivas@elinsa.org

David Diaz Reigosa
University of Oviedo
Gijón, Spain
diazdavid@uniovi.es

***Abstract*— Battery Management Systems (BMS) are key components in battery storage systems in order to guarantee their safe operation and improve their performance, reliability and efficiency. BMS monitor critical parameters in the battery as state-of-charge (SOC), state-of-health (SOH) or temperature. Direct measurement of these parameters is either impossible (e.g. SOC or SOH) or costly and unreliable (e.g. temperature), so they are often estimated. The internal resistor of the battery has already been successfully used to estimate these parameters. BMS can also include the function of balancing (equalizing) cells of a battery pack. Among all available equalizing systems, those based on switched capacitors are interesting due to their simplicity and easy scalability, making them a research focus for several years. This paper proposes an internal resistance (IR) estimation method for LiFePO4 batteries using signals naturally produced by a switched capacitor equalizer (SCE). The method operates online and without interfering with the regular operation of the equalizer.[1]**

Keywords*— *LFP batteries, switched-capacitor equalizer, impedance estimation.

I. Introduction

The use of battery-based Energy Storage Systems (ESS) has highly increased in the last decades [1]. They can be found in a broad range of applications, such as electric vehicles (EV) [1], smart grids [2], aerospace applications [3] and all kind of small appliances applications as mobile devices [4].

There is a wide variety of rechargeable batteries (secondary batteries) technologies that could be used for ESS, as nickel–cadmium (NiCd), Pb-acid or lithium-ion (Li-ion). They all have in common a relatively low voltage, from around 1.2 V in the NiCd to the 3.7 V in some Li-ion with a given chemistry, as $LiMn_2O_4$. Among these, lithium-ion batteries are one of the most attractive batteries for high capacity ESS due to their high energy density, good temperature operation range, low self-discharge and high cell voltage compared with NiCd or Pb-acid [4].

Since the cell voltage in any of these cases is low compared with typical industrial requirements, battery packs are built stacking low voltage cells in series and/or parallel configurations [1]. Manufacturing tolerances, temperature differences, the physical placing of the cells inside the pack, among other reasons, result in voltage imbalances among cells during normal pack operation. These imbalances accelerate aging of cells and result in an increase of the internal battery resistance and in a decrease of its capacity. Mismatches in voltage among cells also increase the internal battery temperature, decreasing therefore operation safety [5]. LIB batteries are generally sensitive to temperature variations. Several parameters, as their Open Circuit Voltage (OCV), capacity or internal resistance can be affect by temperature variations [6]. High temperatures increase the internal resistance and consequently the losses, which can result in thermal runaways and/or explosions. Contrarily, lower temperatures reduce OCV, capacity and internal resistance [7]. In addition, active materials in the Lithium Ion Batteries (LIB) can be potentially damaged in the case of overvoltage [8]. Overvoltage may arise when trying to charge a string of cells when one of the cell has already get to its maximum voltage. Under voltage comes from the reversed case, in which one of the cells has already got to the minimum voltage but the rest can still provide power. For all these reasons, Battery Management Systems (BMS) are needed to monitor critical parameters as temperature, SOC or SOH [2]-[6],[8]-[9], control operational conditions and/or for cell balancing, extending the life of the battery, increasing the overall safety of the system and ensuring a safe range of operation for all the cells forming the pack [9].

Batteries' temperature can be directly measured using temperature sensors [10]. These sensors, although cheap, raise concerns regarding cabling, signal conditioning and acquisition systems, increasing cost, system complexity and the number of elements susceptible of failure [11]. As an alternative, batteries' temperature can be estimated. Temperature estimation methods based on the dependency of the battery IR with its temperature, are the most popular [10], [11]. On the other hand, since SOC and SOH cannot be directly measured, estimation methods must be implemented [9]. Several methods to estimate battery critical parameters can be found in the literature, one of the most popular being based on the battery IR [12]. It can be therefore concluded that battery IR is a reliable metric for temperature, SOC or SOH estimation.

This paper proposes an on-line battery IR estimation, i.e. during cell balancing, for SCEs. The IR of the battery is estimated using signals naturally produced by the SCE. The paper is organized as follows: basis of switched-capacitor equalizers are presented in section II; electrical modeling of

[1] This work was supported in part by the Research, Technological Development and Innovation Programs of the Spanish Ministry Economy and Competitiveness, under grant MINECO-17-ENE2016-80047-R, by the Oviedo Siembra Talento program of the Oviedo City Council and by the Government of Asturias under project IDI/2018/000188 and FEDER funds.

batteries are discussed in section III; the proposed method for battery IR estimation based on SCE is presented in section IV; simulations and experimental results are shown in sections 0 and VI respectively; conclusions are finally presented in section VII.

II. Switched-Capacitor Equalizer

Battery balancing systems extract energy from the most charged cell of a battery pack and either dissipate it or transfer it to a less-charged cell. The first method is known as passive balancing and the second as active balancing. Methods for active balancing can be classified according to different criteria, as the connections between the cells (cell-to-cell, pack-to-cell, cell-to-pack…) or according to the circuit topology (shunting, shuttling or energy conversion methods) [5], [9]. Shunting methods pass the energy from one cell to another without any external energy storage device, unlike shuttling methods that use external energy storage devices, e.g. capacitors, inductors or other batteries. Energy conversion methods use isolated converters for equalizing the cells.

Regarding shuttling active balancing methods, one of the most appealing is the switched capacitor equalizer [13]. This cell-to-cell equalizer balances N cells with N-1 capacitors and 2N switches, see Fig. 1a. The switches continuously work with a fixed duty cycle of 50%, alternating between switches "a" and "b" during regular operation of the battery, including the appropiate dead time to protect the switches from shortcircuits. This can be seen in Fig. 1b, where *Ts* is the switching period and *dt* the dead time. This way, each capacitor is connected half of the switching period in parallel with one cell and the second half with the other one, transferring energy from the one with the highest voltage to the one with the lowest voltage. This is schematically shown in Fig. 1c assuming VB1 > VB2 > VB3. In the state 1, B1 charges C12, i.e. they are connected in parallel, and in state 2, C12 discharges over B2.

Main advantages of this equalizer are that it does not require control, it is fully scalable, cost effective and easy to implement. As a drawback, cells transfer energy effectively only to their adjacent ones, so in certain occasions, e. g. the upper cell has the highest voltage and the lower one the lowest, the energy should flow through all the batteries to get to the less charged one, which increases the losses and the equalization time. The total resistance in the adjacent path includes the battery resistance, the capacitor resistance, two switches and the path itself. There is a path for the energy to flow through non-adjacent cells, however, it is a higher resistive path; to go from B1 to B3 in Fig. 1c, there will be 2 capacitors, 3 batteries and the same number of switches, in addition to a longer path, increasing the total resistance. This means that the resistance increases with the distance between cells, therefore decreasing the amount of energy flowing through non-adjacent cells [14]. A prototype for a SCE to balance four cells is shown in Fig. 1d, this prototype will be used for the experimental verification of the proposed battery IR estimation method.

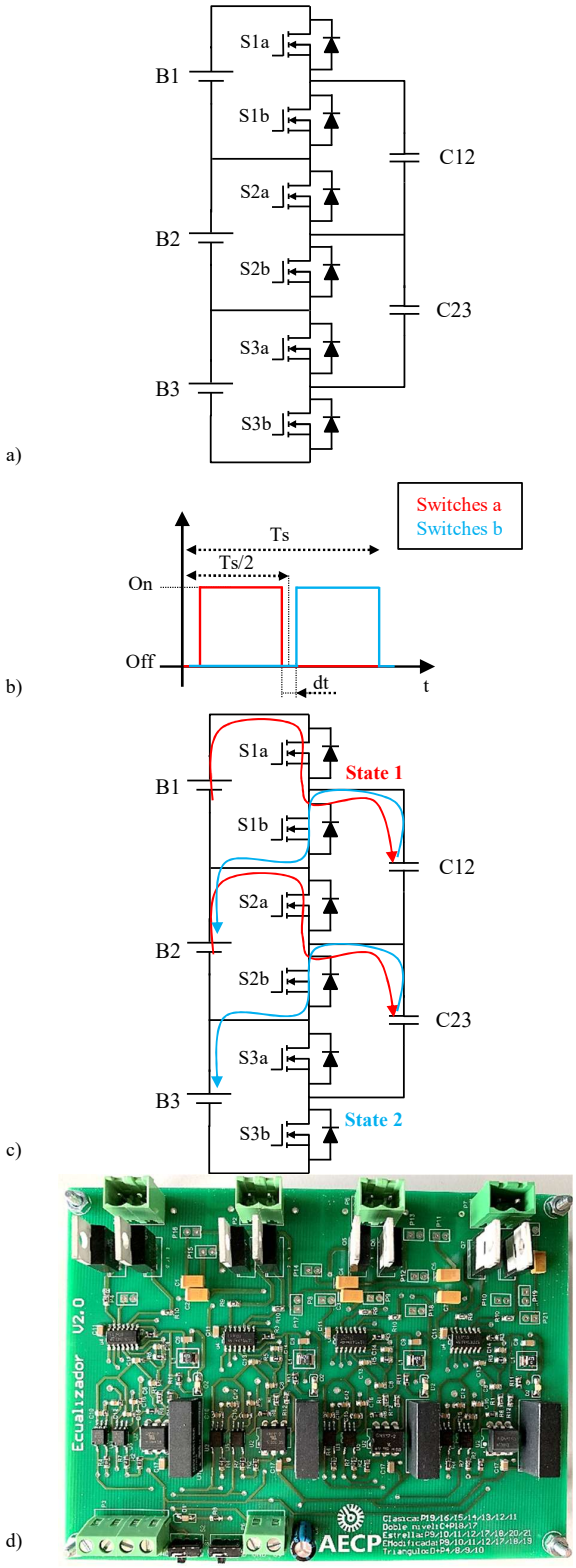

Fig. 1.- Switched capacitor equalizer with 3 batteries, a) schematic with 3 cells, b) switching function, c) paths for the energy at both switching state, d) prototype for balancing up to 4 cells.

A. Switched-Capacitor equalizer topologies

Since this first design, different topologies have been proposed to improve the original topology, see Fig. 1a, in terms of efficiency and equalization time. They all share the same control structure: open loop control with 50% duty cycle. The most relevant ones are the following:

-Double-tiered switched-capacitor equalizer [14]-[16]:Fig. 2. An extra capacitor bridges the capacitors in the first row,

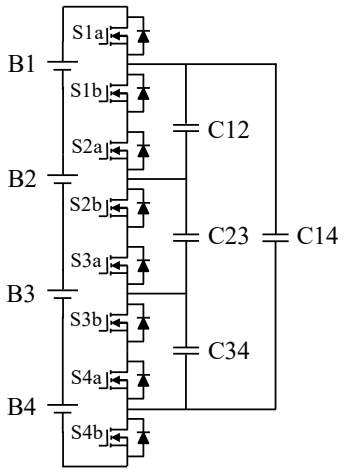

Fig. 2.- Double-tiered switched-capacitor equalizer.

so batteries have two paths to exchange charge, reducing the equalization time. As a drawback, there is a need of adding an extra capacitor to the system, which must stand the combined voltage of all the capacitors, compromising the scalability of the topology.

-Chain structure using additional switches or capacitors [14]: Fig. 3. Requires four additional switches compared to the double-tired SCE, top and bottom cells become therefore adjacent, forcing them to exchange energy between them and their adjacent cells only, and not with all the cells in the pack as in the previous case. The scalability of this topology is compromised as in the previous case since the voltage that the new switches must stand is the same as the whole battery pack.

-Star-structured switched-capacitor equalizer [15]: Fig. 4 left. It requires one additional capacitor respect to the classic proposal and connects the capacitors in a star-structure that allows interconnection of all the cells at the same time, which increases the equalization time (making it independent of the initial imbalance status of the string) and efficiency. As a drawback, the scalability is again compromised because the voltage that each capacitor must stand is different. A variation of this equalizer with one capacitor less, see Fig. 4 right, and better performance is also proposed in [15] and further analyzed in [17].

-Delta structured switched-capacitor equalizer [18]: Fig. 5. This equalizer adds capacitors in such a way that there is always one connecting any two cells, allowing interconnection of all the cells at the same time. As the double-tired SCE, it maintains the number of switches but increases the number of capacitors (in a higher number) while reducing the equalization time. The voltage that each capacitor must stand is different and dependent on the cells they are bridging.

-Series/parallel switched-capacitor equalizer [19]: Fig. 6. It requires one capacitor more than the classic system but double the switches. It connects all capacitors to the batteries and then all capacitors between them, balancing their charge.

This section presented only the systems based purely on switched capacitors. There are more complex systems that combine inductors and capacitors to improve the performance in terms of speed and losses, such as achieving zero current switching [20]. All topologies discussed in this section are cheap and easy to implement thanks to the absence of control. Although the method that is proposed in this paper is evaluated for the classical topology, see Fig. 1a, it can be extended to any other switched-capacitor topology.

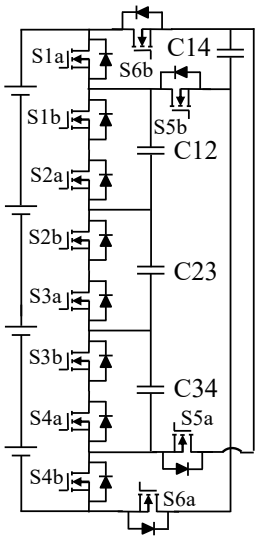

Fig. 3.- Chain structure using additional switches or capacitors.

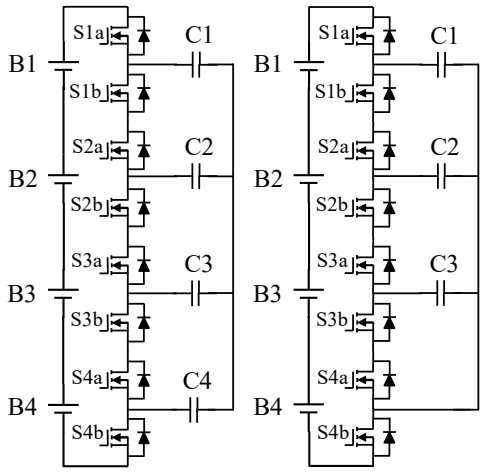

Fig. 4.- Star-structured switched-capacitor equalizer (left) and Star-structured switched-capacitor equalizer (right) with one capacitor less.

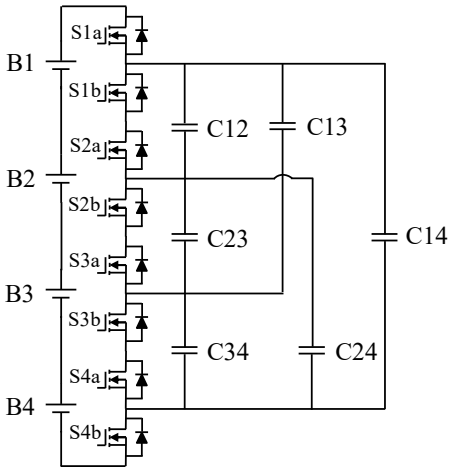

Fig. 5.- Delta-structured switched-capacitor equalizer.

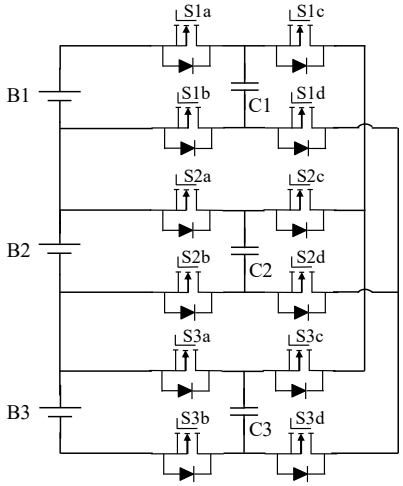

Fig. 6.- Series/parallel switched-capacitor equalizer.

III. Electrical Equivalent Battery Model

There are several ways of modeling the battery behavior: electrochemically (complex and difficult to obtain), mathematically (abstract and application-focused) and electrically (electrical equivalent models based on a combination of electrical elements). The last methods are the most appealing for electrical engineers due to their intuitiveness and ease of use [21]. Among electrical models, the Randles [21], [23], [24] (Fig. 7) and the Thèvenin [21], [22] (Fig. 8) models, are the most commonly used.

The Randles model is obtained from Electrochemical Impedance Spectroscopy (EIS), a standard methodology for battery characterization. It consists of applying AC voltage to the battery and measure the resulting current to estimate the impedance [23], [24]. In Fig. 7a, R_i is the IR, C represents a capacitor holding the cell charge and Zw represents the Warburg impedance which accounts for the diffusion phenomena [23]. Fig. 7b shows the EIS analysis of a LiFePO4 battery.

On the other hand, Thévenin model can be obtained from the battery response to a current step; parameter identification is obtained from the voltage transient response (Fig. 8b) [22]. In Fig. 8b, R_i is the cell IR, R_D and C_D model the dynamic response and C_{SOC} holds the battery charge in this equivalent.

a)

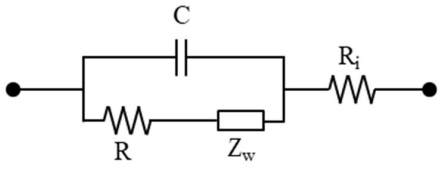

b)

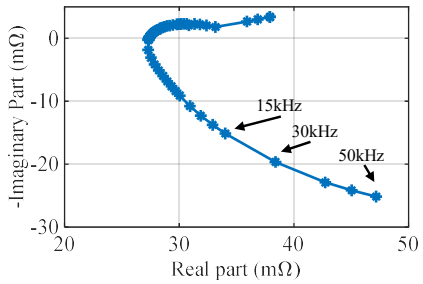

Fig. 7.- Randles equivalent model derived from the Electrochemical Impedance Spectroscopy (EIS) analysis, a) Circuit, b) Nyquist plot.

a)

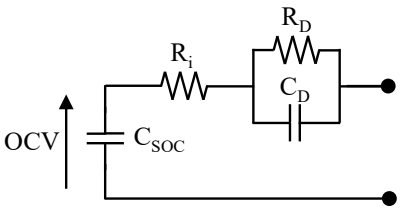

b)

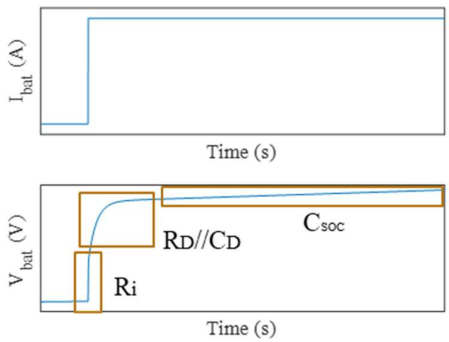

Fig. 8.- Thèvenin equivalent model of a battery, a) Circuit, b) associated step response.

The voltage across C_{SOC} is the OCV of the battery. This capacitor is considered as a voltage source of the same value as the OCV when the battery is modeled at a fixed SOC (i.e. no voltage variations) [21]. The transfer function of this model is shown in (1). The first term on the right hand side of (1) corresponds to the IR, Ri, and is obtained from the initial voltage step, see Fig. 8b, considering the differences in current before and after the step. The second term on the right hand side of (1) is the dynamic RC circuit, a first-order system corresponding to the exponential part of the voltage variation, see Fig. 8b. The last term on the right hand side of (1) is C_{SOC}, a pole at the origin, which accounts for the continuously increasing slope in the voltage in Fig. 8b due to a constant current.

$$G(s) = \frac{V_{bat}}{I_{bat}} = R_i + \frac{R_D}{1 + R_D C_D s} + \frac{1}{s} C_{SOC} \qquad (1)$$

Among these models, the Thévenin one is the most appropriate for battery parameter identification using a SC equalizer, since the process for extracting the parameters involved in (1) (i.e. step response) are analogue to the steps produced in the battery as a result of the SC switching.

IV. Battery Parameter Identification Based on SC Equalizers

This section presents the proposed method for battery IR estimation using signals naturally produced by a SCE. The rest of the paramenters are not of interest for this work. A simplified scheme of an SCE is presented in Fig. 9a, where battery and SCE parameters are shown in Table I. Typical SCE waveforms are shown in Fig. 9b. Note that applying step voltages is analogous to applying step currents for battery parameter estimation [22]. Battery IR, R_i, is obtained from (2), where $v_{bat}(t_i)$ is the voltage value at the instant t_i, 60 µs see Fig. 4b, (3.286 V), $v_{bat}(t<t_i)$ is the voltage value before the connection (3.311 V) and $i_{bat}(t_i)$ is the current value at the instant of the connection (0.508 A). R_i obtained using (2) is ≈50 mΩ, which matches R_i defined in Table I.

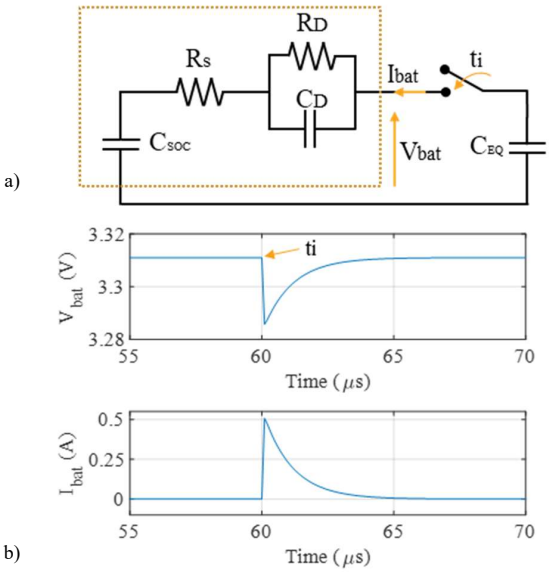

Fig. 9.- a) Simplification of the SCE, modeling the battery as a first order Thèvenin model, and b) voltage and current waveforms of the SCE.

$$R_i = \frac{v_{bat}(t < t_i) - v_{bat}(t_i)}{i_{bat}(t_i)} \quad (2)$$

TABLE I. BATTERY PARAMETERS

Parameter	Value	Parameter	Value
R_i	50 mΩ	C_{SOC}	19 kF
R_D	6.7 mΩ	C_{EQ}	22 µF
C_D	48F		

V. Simulations

An SCE with two cells was implemented in Matlab/Simulink, see Fig. 10. The equalizer main parameters are shown in Table II. Cells are implemented using the battery model from Simscape library, with $LiFePO_4$ battery equivalent parameters. A 30% difference in SOC between batteries is set as initial condition.

TABLE II. EQUALIZER AND BATTERY CHARACTERISTIC PARAMETERS.

Parameter	Value
Nominal battery voltage	3.2 V
Nominal current	3.2A
Maximum charge current	1C
Maximum discharge current	3C
Battery capacity	3300mAh
Equalizer capacitor	22 µF
Internal resistance (R_i)	50 mΩ

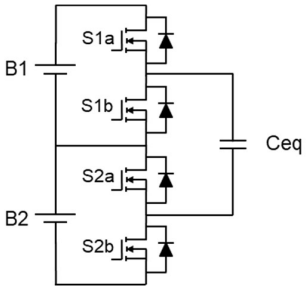

Fig. 10.- Simplification of the SCE.

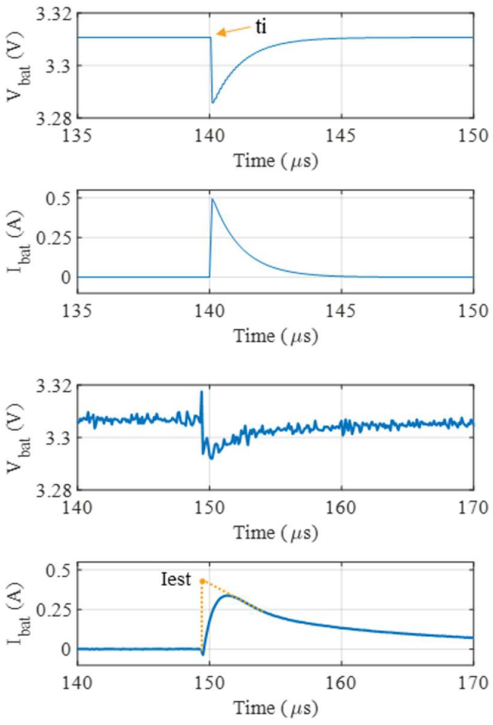

Fig. 11.- Resulting waveform from the equalizer, a) Simulink, b) Experimental results (fs = 20kHz, T=20ºC, SOC differences = 30%).

Fig. 11a shows the voltage and current of the battery when the most charged battery and the balancing capacitor are connected at t=140µs. The simulation results are in good agreement with the ones obtained with the Thèvenin model shown in Fig. 9b. The estimated internal battery resistance (2) is ≈50 mΩ, which matches R_i defined in Table II and included in the battery model for the simulation.

VI. Experimental Results

The SCE shown in Fig. 1c was used to carry out the experimental results. A two cells arrangement has been used to be consistent with the simulation results shown in Section V. Parameters of the battery and SCE are shown in Table II. The $LiFePO_4$ battery used in this work is shown in Fig. 12.

Battery voltage and current in one switching cycle are shown in Fig. 11b. It can be seen the current has a smoother profile than in simulation (Fig. 11a), due to inductive parasitic components present in the real system. This should be compensated for IR estimation. Using the current slope, the ideal current peak can be estimated, see I_{est} in Fig. 11b, (2) can be expressed therefore as (3) where I_{est} is the estimated current.

$$R_i = \frac{v_{bat}(t < t_i) - v_{bat}(t_i)}{I_{est}} \quad (3)$$

Fig. 12.- $LiFePO_4$ battery.

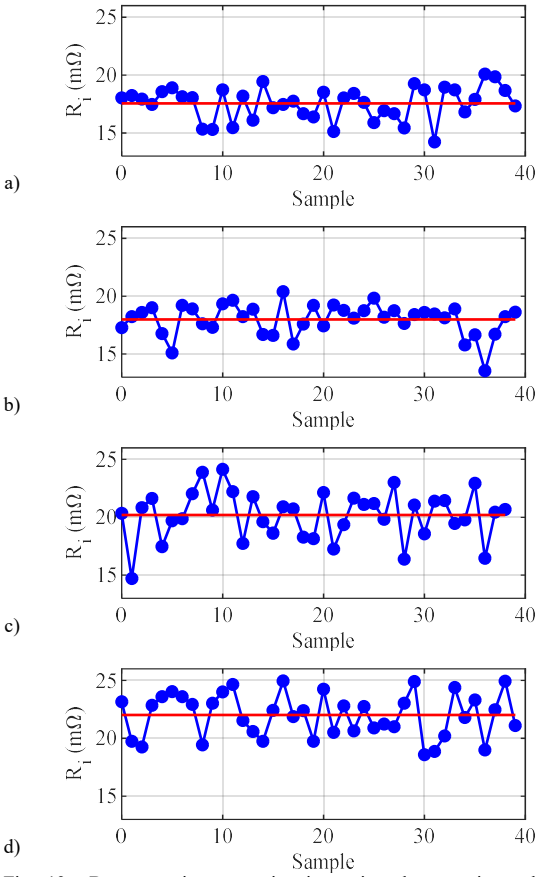

Fig. 13.- Battery resistance estimation using the experimental data collected from the equalizer (blue) and mean value of the estimated resistance (red), a) 5kHz, b) 10kHz, c) 20kHz, d) 50kHz.

Fig. 13 shows the estimated battery resistance for a set of experimental data captured with the SCE working at 5kHz, 10kHz, 20kHz and 50kHz, and the mean value of the estimated battery resistance.

The mean value of the estimated resistances shown in Fig. 13, is shown in Fig. 14a. The mean value of the IR increases with the frequency, as expected from Fig. 7b. It is noted that SOC, SOH or temperature time constants are significantly larger than battery resistance estimation time [25], meaning that averaging the measurements for a certain period of time could be an acceptable and easy solution to reject measurement noise. Experimental results repeated with another battery with the same characteristics to show the replicability of the methodology are shown in Fig. 14b. As it can be seen, the variation with frequency is similar for both cases. However, the range of resistance variation is different. The frequency at 5Khz is around 18 mΩ for the first battery, while it is around 35 mΩ for the second one. This is in agreement with what was said in section I: due to differences between batteries, there is a need of an equalizer in order to avoid differences in voltages, because the batteries with a higher resistance will discharge sooner.

VII. Conclusions

This paper proposes the use of signals naturally produced by SCE to estimate cell battery IR. The method operates without interfering with the regular operation of the equalizer. Experimental results have been provided to demonstrate the viability of the proposed method. This IR estimated could be potentially used to determine other important parameters in a battery, as its temperature.

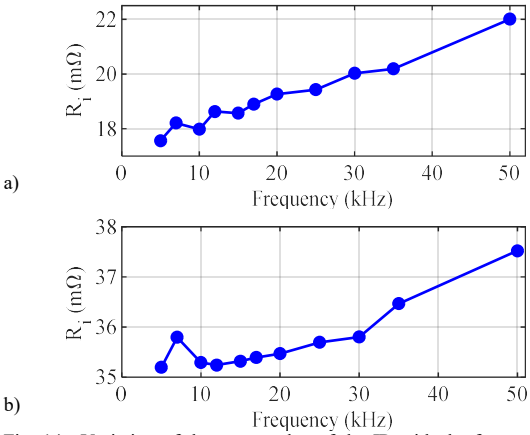

Fig. 14.- Variation of the mean value of the IR with the frequency, a) battery 1 and b) battery 2.

References

[1] D. Anseán, M. González, V. M. García, J. C. Viera, J. C. Antón and C. Blanco, "Evaluation of LiFePO4 batteries for electric vehicle applications," IEEE Transaction on Industrial Application, vol. 51, no. 2, pp. 1855-1863, March-April 2015.

[2] Z. Miao, L. Xu, V. R. Disfani and L. Fan, "An SOC-based battery management system for microgrids," IEEE Transactions on Smart Grid, vol. 5, no. 2, pp. 966-973, March 2014.

[3] J.P. Fellner, G.J. Loeber, S.P. Vukson, C.A. Riepenhoff, "Lithium-ion testing for spacecraft applications," Journal of Power Sources, vol. 119–121, pp. 911-913, June 2003.

[4] Gianfranco Pistoia, "In battery operated devices and systems," Elsevier, Amsterdam, 2009.

[5] J. Cao, N. Schofield and A. Emadi, "Battery balancing methods: A comprehensive review," IEEE Vehicle Power and Propulsion Conference, Harbin, pp. 1-6, Sept. 2008.

[6] A. E. Mejdoubi, H. Gualous, H. Chaoui and G. Alcicek, "Experimental investigation of calendar aging of lithium-ion batteries for vehicular applications," EMC Conference, Turkiye, Ankara, pp. 1-5, Sept. 2017.

[7] C. Alaoui, "Solid-State Thermal Management for Lithium-Ion EV Batteries," IEEE Transactions on Vehicular Technology, vol. 62, no. 1, pp. 98-107, Jan. 2013.

[8] S. W. Moore and P. J. Schneider, "A review of cell equalization methods for lithium ion and lithium polymer battery systems," SAE Technical Paper, March 2001.

[9] H. Rahimi-Eichi, U. Ojha, F. Baronti and M. Chow, "Battery management system: An overview of its application in the smart grid and electric vehicles," IEEE Industrial Electronics Magazine, vol. 7, no. 2, pp. 4-16, June 2013.

[10] R. R. Richardson, P. T. Ireland, D. A. Howey, "Battery internal temperature estimation by combined impedance and surface temperature measurement," Journal of Power Sources, vol. 265, pp. 254-261, Nov. 2014.

[11] C. G. Moral, D. Fernandez, J. M. Guerrero, D. Reigosa and F. Briz, "Thermal monitoring of LiFePO4 batteries using switching harmonics," IEEE Energy Conversion Congress and Exposition (ECCE), Portland, OR, pp. 2734-2740, Sept. 2018.

[12] D. Ansean, M. Gonzalez, J. C. Viera, V. M. Garcia, J. C. Alvarez and C. Blanco, "Electric vehicle Li-Ion battery evaluation based on internal resistance analysis," IEEE Vehicle Power and Propulsion Conference (VPPC), Coimbra, pp. 1-6, Oct. 2014.

[13] C. Pascual and P. T. Krein, "Switched capacitor system for automatic series battery equalization," Proc. IEEE 1997 Applied Power Electronics Conference, pp. 848-854, Feb. 1997.

[14] M. Kim, C. Kim, J. Kim and G. Moon, "A Chain structure of switched capacitor for improved cell balancing speed of Lithium-Ion batteries," IEEE Transactions on Industrial Electronics, vol. 61, no. 8, pp. 3989-3999, Aug. 2014.

[15] Y. Ye, K. W. E. Cheng, Y. C. Fong, X. Xue and J. Lin, "Topology, modeling, and design of switched-capacitor-based cell balancing

systems and their balancing exploration," IEEE Transactions on Power Electronics, vol. 32, no. 6, pp. 4444-4454, June 2017.
[16] A. C. Baughman and M. Ferdowsi, "Double-tiered switched-capacitor battery charge equalization technique," IEEE Transactions on Industrial Electronics, vol. 55, no. 6, pp. 2277-2285, June 2008.
[17] Y. Shang, N. Cui, B. Duan and C. Zhang, "Analysis and optimization of star-structured switched-capacitor equalizers for series-connected battery strings, " IEEE Transactions on Power Electronics, vol. 33, no. 11, pp. 9631-9646, Nov. 2018.
[18] Y. Shang, C. Zhang, N. Cui and C. C. Mi, "A delta-structured switched-capacitor equalizer for series-connected battery strings," IEEE Transactions on Power Electronics, vol. 34, no. 1, pp. 452-461, Jan. 2019.
[19] Y. Ye and K. W. E. Cheng, "Modeling and analysis of series–parallel switched-capacitor voltage equalizer for battery/supercapacitor strings," IEEE Journal of Emerging and Selected Topics in Power Electronics, vol. 3, no. 4, pp. 977-983, Dec. 2015.
[20] Y. Yuanmao, K. W. E. Cheng and Y. P. B. Yeung, "Zero-current switching switched-capacitor zero-voltage-gap automatic equalization system for series battery string," IEEE Transactions on Power Electronics, vol. 27, no. 7, pp. 3234-3242, July 2012.
[21] Min Chen and G. A. Rincon-Mora, "An accurate electrical battery model capable of predicting runtime and I-V performance," IEEE Transactions on Energy Conversion, vol. 21, no. 2, pp. 504-511, June 2006.
[22] B. Schweighofer, K. M. Raab and G. Brasseur, "Modeling of high power automotive batteries by the use of an automated test system," IEEE Transactions on Instrumentation and Measurement, vol. 52, no. 4, pp. 1087-1091, Aug. 2003.
[23] B. Pattipati, C. Sankavaram and K. Pattipati, "System Identification and Estimation Framework for Pivotal Automotive Battery Management System Characteristics," IEEE Transactions on Systems, Man, and Cybernetics, Part C (Applications and Reviews), vol. 41, no. 6, pp. 869-884, Nov. 2011.
[24] S. Buller, M. Thele, E. Karden, R. W. D. Doncker, "Impedance-based non-linear dynamic battery modeling for automotive applications," Journal of Power Sources, vol. 113, no. 2, pp. 422-430, Jan. 2003.
[25] Yuan Zou, Xiaosong Hu, Hongmin Ma, Shengbo Eben Li, "Combined State of Charge and State of Health estimation over lithium-ion battery cell cycle lifespan for electric vehicles," Journal of Power Sources, Volume 273, pp. 793-803, Jan. 2015.